

Kinetic Properties of Chitinase-1 from the Fungal Pathogen *Coccidioides immitis*[†]Tamo Fukamizo,[‡] Chiye Sasaki,[‡] Elisabeth Schelp,[§] Kara Bortone,[§] and Jon D. Robertus^{*,§}

Institute of Cellular and Molecular Biology, Department of Chemistry and Biochemistry, University of Texas, Austin, Texas 78712, and Department of Food Science and Nutrition, Kinki University, 3327-204 Nakamachi, Nara 631-8505, Japan

Received July 5, 2000; Revised Manuscript Received December 21, 2000

ABSTRACT: The endochitinase from *Coccidioides immitis* (CiX1) is a member of the class 18 chitinase family. Here we show the enzyme functions by a retaining catalytic mechanism; that is, the β -conformation of the chitin substrate linkages is preserved after hydrolysis. The pattern of cleavage of *N*-acetylglucosamine (GlcNAc) oligosaccharide substrates has been determined. (GlcNAc)₆ is predominantly cleaved into (GlcNAc)₂ and (GlcNAc)₄, where the (GlcNAc)₂ group arises from the nonreducing end of the substrate and is formed as the β -anomer. With time, transglycosylation occurs, generating (GlcNAc)₈ from the product dimer and fresh hexamer. Similar patterns are seen for the cleavage of (GlcNAc)₅ and (GlcNAc)₄ where dimers cleaved from the nonreducing end reflect the most common binding and hydrolysis pattern. Intrinsic fluorescence measurements suggest the dissociation constant for (GlcNAc)₄ is 50 μ M. Synthetic substrates with fluorescent leaving groups exhibit complicated profiles in the relationship between initial velocity and substrate concentration, making it difficult to obtain the values of kinetic constants. An improved theoretical analysis of the time-course of (GlcNAc)₆ degradation allows the unitary free energy of binding of the individual subsites of the enzyme to be estimated. The free energy values obtained are consistent with the dissociation constant obtained by fluorescence measurements, and generate a model of substrate interaction that can be tested against the crystal structure of the enzyme.

Fungi are the causative agent of a wide range of human pathogenesis. One of the most dangerous is *Coccidioides immitis*, which can lead to life-threatening lung infections such as coccidioidomycosis (1). Fungal infections can be particularly dangerous in immuno-compromised patients, like those with HIV infections (2, 3). Chitin, a β -1,4-linked polymer of *N*-acetylglucosamine (GlcNAc),¹ is a major component of fungal cell walls (4). As a consequence, there is interest in analyzing fungal machinery responsible for chitin metabolism including chitin synthases and chitinases as potential antibiotic targets.

C. immitis expresses two chitinases, called CTS1 and CTS2 (5). Cloning of the gene for the principle *Coccidioides* complement fixing antigen, described as the CF/chitinase protein, revealed it to be identical with CTS1 (6). That protein was expressed as a fusion with GST; a thrombin cleavage site in the linker allows for ready purification of the active chitinase from which a target sequence has been removed. To help establish a uniform nomenclature for chitinases, we will refer to the *C. immitis* chitinase-1 molecule as CiX1.

CiX1 is a 427 residue protein which is both found in the cytoplasm and expressed on the cell surface, consistent with its antigenicity. Based on the amino acid sequence, the enzyme is a member of glycohydrolase family 18 (7). This is a large family of chitinases, with representatives from fungi, bacteria, higher plants, and animals. We have recently solved the X-ray structure of the chitinase at 2.2 Å (8). The structure of CiX1 and the other class 18 chitinases is very different from that of the class 19 chitinases (9). The class 19 enzymes have a protein fold similar to that of lysozymes, and have inverting mechanisms of action (10). As part of our complete structural analysis of CiX1, we are investigating the catalytic mechanism of the enzyme. Here we report the use of oligosaccharides and artificial substrates to measure the enzyme's kinetic parameters.

MATERIALS AND METHODS

Materials. The enzyme was purified from a fusion with glutathione *S*-transferase (GST) (6) as described previously (11). Briefly, the GST–CiX1 fusion was grown in *E. coli*, purified by binding to a glutathione column, and the active chitinase fragment was released by thrombin hydrolysis.

pH–Activity Profile. Optimal pH for the enzyme was determined using 4-methylumbelliferyl β -*N,N'*-diacetylchitobioside [(GlcNAc)₂-4MU] (Sigma). A (GlcNAc)₂-4MU solution (250 μ M) was prepared in 45 mM sodium citrate, 45 mM potassium phosphate, 45 mM Tris buffer at half pH unit intervals ranging from pH 3 to pH 9. The substrate solution (340 μ L) was incubated with 85 μ L of enzyme (4 mg/mL) at 30 °C. One hundred microliter aliquots were removed from the reaction mixture at 0, 1, 2, and 3 h and

[†] This work was supported by grants from the National Institutes of Health (GM 30048), the Foundation for Research, and the Welch Foundation.

* Correspondence should be addressed to this author at the Institute of Cellular and Molecular Biology, Department of Chemistry and Biochemistry, University of Texas, Austin, TX 78712. Tel: 512-471-3175, Fax: 512-471-6135, E-mail: jrobertus@mail.utexas.edu.

[‡] Kinki University.

[§] University of Texas.

¹ Abbreviations: GlcNAc, *N*-acetylglucosamine; (GlcNAc)₃-4MU, 4-methylumbelliferyl β -*N,N',N''*-triacylchitotriose; (GlcNAc)₂-4MU, 4-methylumbelliferyl β -*N,N'*-diacetylchitobiose.

stopped in 5.9 mL of 0.5 M glycine, pH 10.4. Release of free 4-methylumbelliferone was measured by fluorescence spectroscopy using a Turner model 450 fluorometer, exciting at 360 nm and measuring emission at 450 nm. Subsequent enzyme assays were performed in 0.1 M potassium phosphate buffer at pH 7.0. Steady-state kinetic measurements against (GlcNAc)₂-4MU and (GlcNAc)₃-4MU were carried out in a similar fashion; substrate concentrations were varied from 0 to 250 μ M.

HPLC Determination of Product Anomers. The anomeric form of the products was determined by HPLC, and the cleavage pattern was assessed from the anomer formation (12). The enzymatic hydrolysis of the substrate was carried out in 0.1 M sodium phosphate buffer, pH 6.0 at 25 °C. Concentrations of the enzyme and various substrates were 2.6 μ M and 2.7 mM, respectively. The substrate degradation and product formation were followed by HPLC analysis using a TSK Amide 80 column. The elution solvent was 70% acetonitrile, and the flow rate was 0.7 mL/min; oligosaccharides were detected by ultraviolet absorption at 220 nm.

HPLC Determination of the Reaction Time-Course. Time-courses for (GlcNAc)_n hydrolysis catalyzed by *C. immitis* chitinase were followed by gel filtration. The enzymatic reaction was done in 0.1 M sodium phosphate buffer, pH 6.0 and 40 °C. Substrate concentrations were 4.3 mM for hexamer, 5.5 mM for pentamer, and 5.8 mM for tetramer. Enzyme concentration was 0.7 μ M in each experiment. The substrate degradation and product formation were followed by gel filtration analysis using a TSK-GEL G2000PW column. The elution solvent was distilled water, and the flow rate was 0.3 mL/min. The oligosaccharides were detected by ultraviolet absorption at 220 nm.

Equilibrium Binding Experiments with (GlcNAc)₄. A binding curve was obtained for (GlcNAc)₄ by measuring the change in intrinsic fluorescence of 1 mM chitinase while titrating with ligand at pH 8.5 and 4 °C. Measurements were made by exciting at 290 nm and measuring fluorescence emission at 340 nm using an SLM 8000 fluorescence spectrophotometer. Final titration of the ligand did not exceed 5% of the starting volume. To make hydrolysis of ligand a negligible factor, titration and fluorescence measurements were completed in less than 5 min. As a control, ligands were also treated with 11 mM free tryptophan, and a fluorescence scan was taken, exciting at 290 nm and measuring emission between 310 and 400 nm. The free tryptophan and (GlcNAc)₄ together showed a slightly lower fluorescence than free tryptophan alone.

Theoretical Calculation of the Reaction Time-Course. Theoretical analysis of the reaction time-course was carried out using the reaction model reported for hen egg white lysozyme (13). A slight modification has been introduced in that we assumed that CiX1 has subsites for sugar binding of the form: (-2)(-1)(+1)(+2)(+3)(+4). To estimate the values of unitary binding free energy changes of individual subsites, and rate constant values k_{+1} , k_{-1} , and k_{+2} (see Figure 6), an optimization technique based on the modified Powell method (14) was employed using the cost function:

$$F = \sum_i \sum_n [(GlcN)calc_{n,i} - (GlcN)exp_{n,i}]^2 \quad (1)$$

where *exp* and *calc* are the experimental and calculated

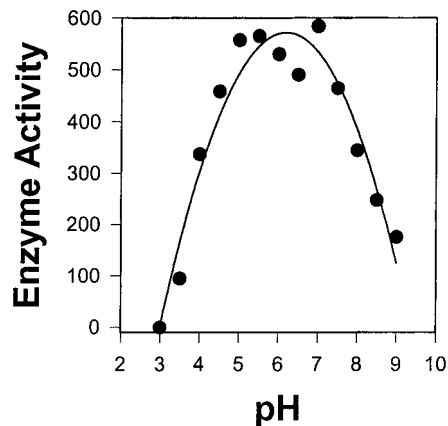


FIGURE 1: pH versus activity profile for CiX1. The activity was measured by release of fluorescent methylumbelliferone from (GlcNAc)₂-4MU.

values, n is the size of the oligosaccharides, and i is the reaction time. In the calculation of the time-course, the rate constant value of k_{+1} (for cleavage of the glycosidic linkage) was assumed to be dependent upon the substrate size (13).

RESULTS

pH Dependence. Figure 1 shows the activity of CiX1 as a function of pH; the substrate is (GlcNAc)₂-4MU. The optimum pH is about 6.0. Plots of the log of activity versus pH (not shown) were difficult to interpret in the classical sense. The slope of the low-pH limb of the plot was 1, suggesting activity is controlled by a single group with a pK_a of 4.5. The high-pH limb of the plot had a slope of 0.33, indicating a complex response to pH which is not readily interpreted.

Anomeric Form of the Reaction Products. The anomers of CiX1 products from (GlcNAc)₆ substrate were determined using HPLC. The top of Figure 2 shows a mutarotation equilibrium standard for GlcNAc and for the oligomers through pentamers. In each case, the equilibrium ratio of α : β anomer was found to be about 5:2. The bottom of Figure 2 shows the major CiX1 hydrolysis products from (GlcNAc)₆ at pH 6.0. The major products are (GlcNAc)₂ and (GlcNAc)₄, and the two anomers of each product elute separately as a function of time. The ratio of α : β in the reaction product (GlcNAc)₂ was about 1:9 after 5 min of the reaction time; that is, the newly formed disaccharide is largely β . In contrast, the ratio of α : β for the (GlcNAc)₄ product was 5:2, similar to that in the standard mutarotation equilibrium. As reaction time increases to 60 min, the anomeric ratio for (GlcNAc)₂ is about 1:2 as the sugar mutarotates toward the predominant equilibrium α form. The ratio for (GlcNAc)₄ remains constant at 5:2 even after 60 min. A very small amount of (GlcNAc)₃ was also produced, and the ratio of α : β of the product was about 1:1. This is consistent with some cleavage to form (GlcNAc)₃ + (GlcNAc)₃ where the trimer with the newly created reducing end is largely β and the other is mostly α . Despite some buffer perturbation at the elution position for GlcNAc, it is clear that GlcNAc was hardly produced by this enzyme.

Reaction Time-Course. In separate experiments, the rate of product formation for various oligosaccharide substrates was followed by HPLC as a function of time. Figure 3a shows the loss of (GlcNAc)₆ and the formation of other

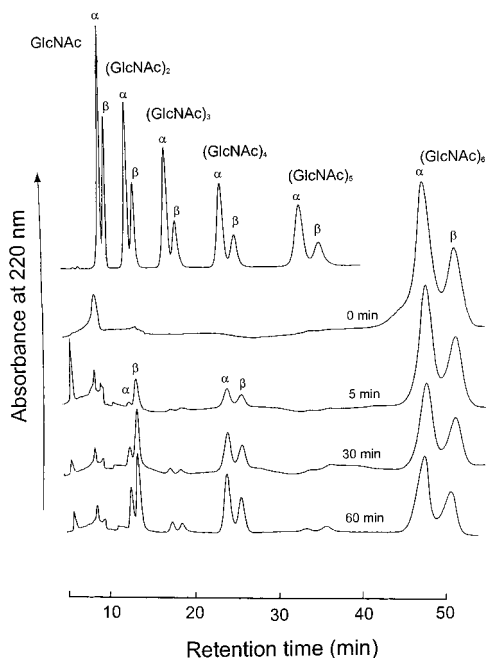


FIGURE 2: HPLC separation of GlcNAc oligomers. The trace at the top of the figure shows the separation of monomer through pentamer derivatives of GlcNAc; under these conditions, the α anomers are separated from the β as labeled. Below these standards are the traces from the time-dependent hydrolysis by CiX1 of (GlcNAc)₆. The traces represent samples taken at 0, 5, 30, and 60 min intervals as labeled. The α and β anomers of the di- and tetrasaccharide products have been labeled on the 5 min trace.

oligosaccharides. As before, (GlcNAc)₆ was hydrolyzed mainly to (GlcNAc)₂ + (GlcNAc)₄ with much less cleavage to form (GlcNAc)₃ + (GlcNAc)₃. There is also indication of the transglycosylation products, such as (GlcNAc)₈. This can arise after the accumulation of products as the condensation of two tetramers or of a dimer with a hexamer. The initial turnover of the enzyme against 4 mM hexamer is about 30 min⁻¹ as measured by the loss of hexamer.

The hydrolysis of (GlcNAc)₅ is shown in Figure 3b and that of (GlcNAc)₄ in Figure 3c. The pentamer is cleaved primarily to trimers and dimers, with some transglycosylation to heptamer (pentamer + dimer). (GlcNAc)₄ is cleaved

almost exclusively to dimers, but some transglycosylation to hexamers is observed.

Initial Velocity as a Function of Substrate Concentration. We next investigated the steady-state kinetics of substrate hydrolysis by CiX1. Initial velocities of the tetramer (GlcNAc)₄ hydrolysis as a function of the substrate concentration are shown in Figure 4a. The profile is clearly not the rectangular hyperbola expected of standard Michaelis–Menten kinetics. The velocity is inhibited as the substrate concentration increases above 1 mM. Normal K_m and k_{cat} values cannot be calculated with confidence, but it is reasonable to assume that the linear velocity increase at low substrate concentrations allows the specificity constant (k_{cat}/K_m) to be measured as the initial slope of the velocity curve. This reveals a value of about $6 \times 10^4 \text{ M min}^{-1}$ for (GlcNAc)₄.

We also observed the hydrolysis of the unnatural fluorescent substrates (GlcNAc)₂-4MU and (GlcNAc)₃-4MU. The release of fluorescent product was monitored over time and the velocity measured in the linear range. Initial velocities are plotted as a function of substrate concentrations in Figure 4b. The kinetics are, again, clearly not hyperbolic. The specificity constants are about $1 \times 10^6 \text{ M min}^{-1}$ for (GlcNAc)₂-4MU and $0.7 \times 10^6 \text{ M min}^{-1}$ for (GlcNAc)₃-4MU. We also tested the chitinase from *Serratia marcescens* as seen in Figure 4b. Like CiX1, this enzyme showed strong substrate inhibition with (GlcNAc)₃-4MU and showed a specificity constant of $0.8 \times 10^6 \text{ M min}^{-1}$. Direct data-fitting to the substrate inhibition profiles was not successful with any substrate inhibition models including a 1:2 or 1:3 enzyme–substrate complex.

Binding Experiment with (GlcNAc)₄. We measured the change in intrinsic fluorescence of CiX1 as a function of added (GlcNAc)₄ concentration at pH 8.5. Because the time lapse in the measurement is short, and enzyme activity was reduced at pH 8.5, there is little hydrolysis of the tetrasaccharide during these measurements. The data are shown in Figure 5. CiX1 appears to be half-saturated when the concentration of (GlcNAc)₄ is about 50 μM , and this may be taken as a measure of the dissociation constant for this substrate.

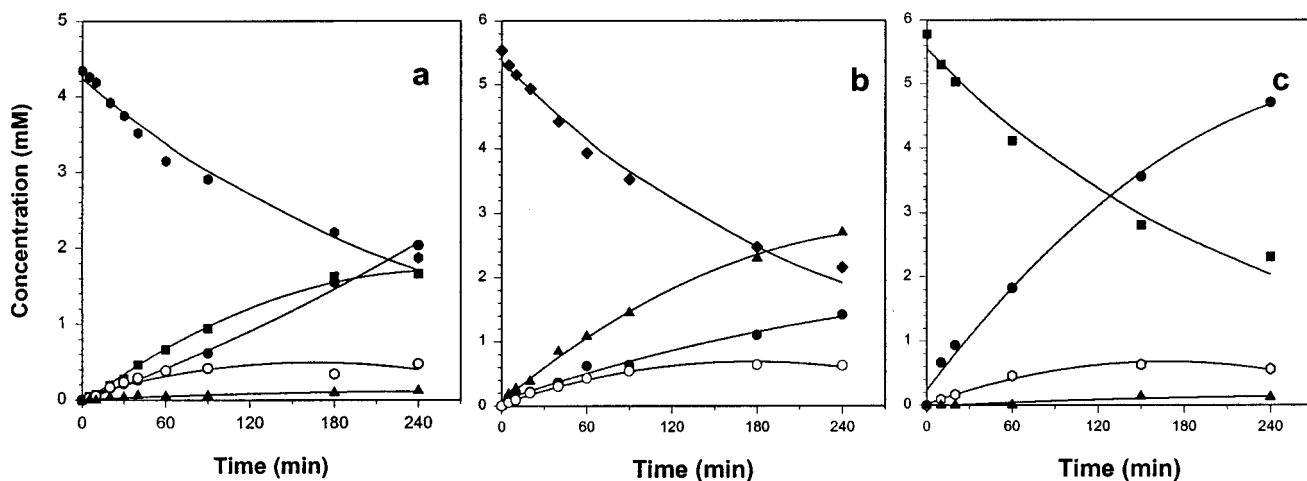


FIGURE 3: Time-courses of GlcNAc oligosaccharide hydrolysis by CiX1. Panel A shows the hydrolysis of (GlcNAc)₆. Hexamers are shown as filled hexagons, dimers as filled circles, trimers as filled triangles, and tetramers as filled squares. Octamers generated by transglycosylation are shown as open circles. In panel B, (GlcNAc)₅ is shown as filled diamonds, dimers as filled circles, trimers as filled triangles, and heptamers as open circles. In panel C, (GlcNAc)₄ is shown as filled squares, dimers as filled circles, trimers as filled triangles, and hexamers formed by transglycosylation as open hexagons.

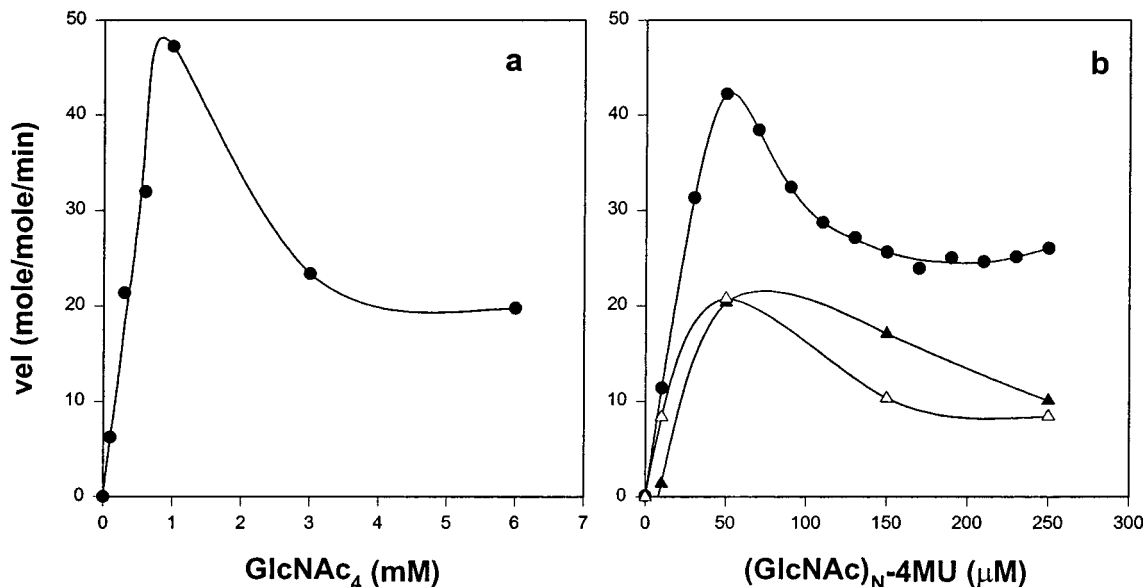


FIGURE 4: Relationship between initial velocity and substrate concentration. Panel a: $(\text{GlcNAc})_4$ hydrolysis by CiX1. Panel b: $(\text{GlcNAc})_n$ -4MU ($n = 2$ or 3) hydrolysis by CiX1. The hydrolysis of $(\text{GlcNAc})_2$ -4MU by CiX1 is shown as solid circles, and the hydrolysis of $(\text{GlcNAc})_3$ -4MU by CiX1 is shown as solid triangles. Hydrolysis of $(\text{GlcNAc})_3$ -4MU by chitinase from *S. marcescens* is shown as open triangles.

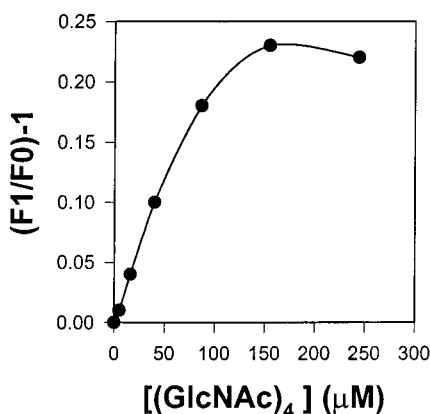


FIGURE 5: Intrinsic fluorescence of CiX1 as a function of $(\text{GlcNAc})_4$ concentration. The enzyme is half-saturated at an approximately $50 \mu\text{M}$ aliquot of the tetrasaccharide. The symbols are the same as in Figure 4a.

Theoretical Analysis of the Reaction Time-Course. To obtain key kinetic constants, we tried to directly analyze the reaction time-course shown in Figure 3 with the reaction model shown in Figure 6. The subsite nomenclature for CiX1 is based on suggested conventions (15). Initially, the rate-limiting step was assumed to be k_{+1} and was estimated from Figure 3 as 0.60 s^{-1} for $(\text{GlcNAc})_4$, 0.60 s^{-1} for $(\text{GlcNAc})_5$, and 0.52 s^{-1} for $(\text{GlcNAc})_6$. The k_{-1} value was set at the value estimated for hen egg white lysozyme (13), 40.0 s^{-1} . A higher value, 200.0 s^{-1} , was tentatively allocated to k_{+2} . The unitary free energy values at individual subsites were roughly estimated from the $(\text{GlcNAc})_6$ cleavage pattern assessed from the HPLC profiles shown in Figure 3. Following the example of barley chitinase (16), the free energy value of site (-1) was set at an unfavorable positive value, $+4.5 \text{ kcal/mol}$. A positive value was also allocated to the free energy value at subsite (+3), because the $(\text{GlcNAc})_6$ hydrolysis into $(\text{GlcNAc})_3 + (\text{GlcNAc})_3$ is not as frequent as those into $(\text{GlcNAc})_2 + (\text{GlcNAc})_4$ and $(\text{GlcNAc})_4 + (\text{GlcNAc})_2$. Thus, the initial estimates of free

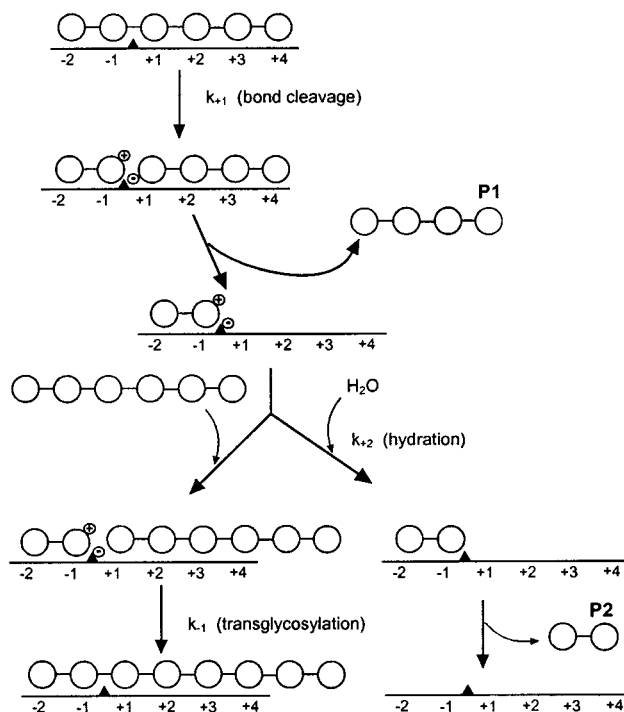


FIGURE 6: Reaction model scheme of CiX1-catalyzed hydrolysis and transglycosylation. Sugar binding subsites are labeled (-2) to (+4), and hydrolysis occurs between sites (-1) and (+1). The charged oxazoline intermediate is indicated by a + charge and the deprotonated catalytic acid of the enzyme, Glu 171, by a - charge. A simultaneous differential equation of formation and degradation of individual chitoooligosaccharides was derived from this model, and numerically solved to obtain the theoretical time-course. In the practical calculation, all possible binding modes of the saccharides are taken into consideration [Fukamizo et al. (13)].

energy values were set at $-3.0, +4.5, -3.0, -3.0, +0.5,$ and -3.0 kcal/mol for individual subsites. The value -3.0 kcal/mol is the average value of lysozyme subsites except subsite (-1), which has a positive free energy value, $+4.5 \text{ kcal/mol}$ (17). Starting from these initial estimates, optimization was carried out changing the unitary free energy values,

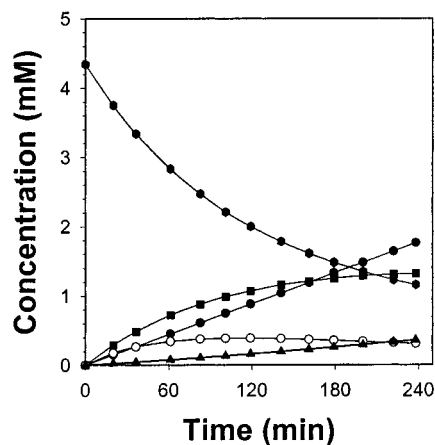


FIGURE 7: Theoretical time-course obtained by numerically solving the differential equation derived from the reaction model scheme shown in Figure 6. The values of the kinetic parameters used in this calculation are listed in Table 1.

Table 1: Kinetic Parameters Estimated from the Theoretical Analysis of the Reaction Time-Course

	substrate	rate constant (s^{-1})	binding site energy	
			subsite	kcal/mol
k_{+1}	(GlcNAc) ₆	0.5 ± 0.1	(-2)	-3.8 ± 0.1
	(GlcNAc) ₅	0.6 ± 0.1	(-1)	$+3.1 \pm 0.1$
	(GlcNAc) ₄	1.7 ± 0.1	(+1)	-2.5 ± 0.2
k_{-1}	(GlcNAc) ₆	220 ± 20	(+2)	-3.0 ± 0.4
k_{+2}	(GlcNAc) ₆	200 ± 50	(+3)	$+0.8 \pm 0.4$
			(+4)	-1.8 ± 0.2

while fixing the rate constant values. With -3.8 , $+3.1$, -2.5 , -3.0 , $+0.8$, and -1.8 kcal/mol for the free energy values of individual subsites, the value of the cost function (eq 1) attained a minimum value. In the time-course calculated with these values (not shown), however, discrepancies were found in the production rates of (GlcNAc)₄ and (GlcNAc)₈. To improve these points, optimization was again carried out, changing the values of k_{-1} and k_{+1} for (GlcNAc)₄, while fixing the free energy values at individual subsites. Finally, the time-course calculation with 220 and 1.7 s^{-1} for k_{-1} and k_{+1} values was found to give a much lower value of cost function. The kinetic parameter values finally obtained are listed in Table 1, and the calculated time-course best-fitted is shown in Figure 7.

DISCUSSION

It is generally considered that class 18 chitinases, like CiX1, work through a retaining mechanism of action (18). That is, the β -glycosidic linkage of the chitin substrate is preserved in the product. Our work shows that this is the case for CiX1 (Figure 2). Our studies also indicate that polysaccharides bind to an extended site on CiX1 and are preferentially cleaved between the second and third sugars from the nonreducing end of the substrate. We also see that with time transglycosylation can occur, generating elongated polysaccharides.

It was originally thought that the retaining mechanism might resemble the double displacement mechanism of lysozyme (19), but it now appears that class 18 chitinases function by anchimeric assistance. During catalysis, the carbonyl oxygen of the C2 *N*-acetyl group makes a bond to C1, forming an oxazoline intermediate (20, 21). In this

mechanism, a catalytic acid (22) protonates the leaving group, creating a transient negative charge on the enzyme, while the scissile sugar residue adopts the oxazoline cation structure. We used site-directed mutagenesis to show that Glu171 is the catalytic acid in CiX1 (8).

Many of the catalytic properties of CiX1 are summarized in Figure 6. This shows a hexamer binding in sugar binding sites (-2)~(+4), with the nonreducing end at site (-2). The cleavage site lies between sites (-1) and (+1), that is, the second and third sugars from the nonreducing end. After protonation of the leaving group by Glu171, the enzyme acquires a transient negative charge, and the oxazoline intermediate is cationic. P1, the (GlcNAc)₄ product, can diffuse away. The disaccharide derivative can then be hydrolyzed to create (GlcNAc)₂ that can diffuse out as P2. The newly generated anomeric hydroxyl on (GlcNAc)₂ retains the β conformation.

In some cases, before water can react with the oxazoline intermediate, another polysaccharide, shown in Figure 6 as (GlcNAc)₆, can bind to the leaving group site. It is deprotonated by the Glu171 base, triggering the transglycosylation reaction and creating an elongated polymer. Glycosylation is known in this family of enzymes (23), but the reaction is thermodynamically unfavorable and probably does not occur naturally where products are greatly diluted. In the cell, chitin synthesis is an energy-requiring process in which chitin synthase catalyzes the condensation of UDP-GlcNAc (24).

The cleavage pattern seen for shorter oligosaccharide substrates is similar to that seen for (GlcNAc)₆. (GlcNAc)₅ binds at sites (-2)~(+3) with cleavage between (-1) and (+1) generating the dimers and trimers seen in Figure 3b. Transglycosylation generates heptamers, by joining a dimer in (-2) and (-1) to a fresh pentamer in sites (+1)~(+3). A tetramer would bind in sites (-2)~(+2), and transglycosylation produces hexamers by joining the dimer product at (-2) and (-1) with a fresh tetramer at sites (+1)~(+4).

The hydrolysis of short natural substrates such as (GlcNAc)₄ reveals a complicated steady-state kinetic profile (Figure 4a), suggesting that substrate inhibition is occurring. Similar profiles were obtained, when (GlcNAc)₂-4MU and (GlcNAc)₃-4MU were used as the substrate (Figure 4b). The use of such substrates, which release a fluorescent product, is a common and simple assay for chitinase activity (25, 26). When used as substrates for class 19 chitinases, these artificial substrates exhibit hyperbolic kinetics for which K_m and k_{cat} values can be readily measured (26). However, the simple hyperbolic kinetics were not obtained for CiX1. Substrate inhibition is frequently encountered in endo-type glycosidases, which have a multi-subsite binding cleft, when using low molecular weight oligomers as the substrates (27-29). In most of these cases, a direct data-fitting to the substrate inhibition profiles was successful with substrate inhibition models including a 1:2 or 1:3 enzyme-substrate complex. In CiX1, however, such a direct data-fitting was not successful. The deviation of the theoretical line from the experimental points was intensive especially at the highest substrate concentration region (>5 mM in Figure 4a; >200 μ M in Figure 4b). Thus, the CiX1-catalyzed reaction is likely to involve some unidentified processes complicating the reaction kinetics. Nevertheless, the following information was obtained from the complicated profiles. At 1 mM substrate, CiX1 hydrolyzes about 50 bonds per minute (Figure 4a). This compares

with k_{cat} values for (GlcNAc)₆ hydrolysis of 25 min⁻¹ by the class 19 chitinase from yam (25) and 15 min⁻¹ for hen lysozyme (30). Both of those enzymes operate by a different catalytic mechanism, but the similarity of rates may reflect the difficulty of hydrolyzing β -linked polysaccharides.

The use of (GlcNAc)₂-4MU and (GlcNAc)₃-4MU, which release a fluorescent product, is a common and simple assay for chitinase activity (25, 26). When used as substrates for class 19 chitinases, these artificial substrates exhibit hyperbolic kinetics for which K_m and k_{cat} values can be readily measured (26). As seen in this study for CiX1, and in the analysis of the related chitinase from *S. marcescens* (31), these common synthetic substrates undergo complex reactions with class 18 chitinases. However, at low substrate concentrations, the initial slope can be used to assess the specificity constant, k_{cat}/K_m , and this will allow useful comparisons, for example, between mutant enzyme activities.

As a further effort to obtain the values of kinetic constants, we modeled the reaction time-course of (GlcNAc)₆ hydrolysis, making certain assumptions about substrate binding. In the classical time-course analysis based on the subsite theory, it is assumed that the rate constant values and binding free energy changes are independent (32). Today, however, such an assumption is not acceptable, because it is assumed that substrate occupancy cooperatively affects the catalytic constant and binding free energy of the enzyme. In our time-course analysis, the rate constant of bond-cleavage (k_{+1}) is assumed to be dependent upon the substrate size. As described above, (GlcNAc)₆ binds to (-2)~(+4), (GlcNAc)₅ to (-2)~(+3), and (GlcNAc)₄ to (-2)~(+2). Thus, the substrate size dependence of the rate constant of bond-cleavage can be regarded as an alternative to the subsite occupancy dependence. In fact, the analysis gave a satisfactory fitting of the theoretical lines to the experimental data points (Figure 7) and gave reasonable values for the rate constants and for the free energy of binding individual subsites (Table 1). The cooperativity between the free energy changes of individual subsites appears to be negligibly small in this case. In the case of lysozyme subsites A, B, and C, the binding free energy changes of GlcNAc, (GlcNAc)₂, and (GlcNAc)₃ can be readily explained by assuming additivity of the individual subsite free energies. A similar additivity assumption appears to hold true for the chitinase binding subsites. The quality of the model rate constants can be assessed by comparing the observed hydrolysis of (GlcNAc)₆ shown in Figure 3a with the modeled hydrolysis of Figure 7. The parameter values thus obtained contain some error, as listed in Table 1. The errors for the (+2) and (+3) subsites are relatively large. Nevertheless, the reliability of the estimated values can be confirmed as follows. The (GlcNAc)₄ binding experiments using tryptophan fluorescence showed a dissociation constant of 50 μM . This corresponds to an association constant of $2 \times 10^4 \text{ M}^{-1}$, which can be further converted to a unitary free energy change according to the equation:

$$\Delta G_{\text{u}} = -RT \ln K_{\text{assoc}} - \Delta G_{\text{mix}} \quad (2)$$

$$(\Delta G_{\text{mix}} = RT \ln 55.5)$$

where ΔG_{u} and ΔG_{mix} are unitary and mixing free energy changes of binding, respectively. Thus, we obtained -7.6

kcal/mol for the unitary binding free energy change of (GlcNAc)₄ binding to CiX1. From the cleavage pattern of (GlcNAc)₄ (Figure 4c), the tetrasaccharide binds mainly to sites (-2)~(+2). Assuming the additivity of the free energy values of individual subsites, the free energy change of (GlcNAc)₄ binding to sites (-2)~(+2) can be calculated from the estimated free energy values (Table 1) to be -6.2 kcal/mol, which is comparable to the value obtained from the fluorescence binding curve (Figure 5). Thus, we believe that the free energy values obtained from the theoretical analysis of the reaction time-course are reliable. The unfavorable energy for binding GlcNAc to subsite (-1) presumably reflects the fact that this site is complementary to the oxazoline-like transition state.

The relative efficiency of transglycosylation, k_{-1}/k_{+2} , is 1.1 for CiX1, while the value for hen lysozyme is reported to be 133 (17). In the CiX1-catalyzed reaction, however, the affinity of oligosaccharide to sites (+1)~(+4) is higher than that of hen lysozyme. The higher affinity to sites (+1)~(+4) would compensate the low value of k_{-1}/k_{+2} , resulting in the appreciably high efficiency of transglycosylation.

This is the first fungal chitinase for which an X-ray structure has been determined. Continuing X-ray analysis underway in our laboratory should allow us to identify substrate subsites and to compare substrate binding interactions with the theoretical model presented here. The details of the substrate binding site may then allow the design of fungal enzyme-specific inhibitors that may have utility as antifungal agents.

REFERENCES

1. Cole, G. T., and Kirkland, T. N. (1991) in *The fungal spore and disease initiation in plants and animals* (Cole, G. T., and Hoch, H. C., Eds.) pp 403-443, Plenum Press, New York.
2. Minamoto, G. Y., and Rosenberg, A. S. (1997) *Med. Clin. North Am.* 81, 381-409.
3. Ampel, N. M. (1996) *Emerging Infect. Dis.* 2, 109-116.
4. Bulawa, C. E., and Osmond, B. C. (1990) *Proc. Natl. Acad. Sci. U.S.A.* 87, 7424-7428.
5. Pishko, E. J., Kirkland, T. N., and Cole, G. T. (1995) *Gene* 167, 173-177.
6. Yang, C., Zhu, Y., Magee, D. M., and Cox, R. A. (1996) *Infect. Immun.* 64, 1992-1997.
7. Henrissat, B., and Bairoch, A. (1993) *Biochem. J.* 293, 781-788.
8. Hollis, T., Monzingo, A. F., Bortone, K., Ernst, S., Cox, R., and Robertus, J. D. (2000) *Protein Sci.* 9, 544-551.
9. Robertus, J. D., and Monzingo, A. F. (1999) in *Chitin and chitinases* (Jolles, P., and Muzzarelli, R. A. A., Eds.) pp 125-135, Birkhauser Verlag, Basel, Switzerland.
10. Monzingo, A. F., Marcotte, E. M., Hart, P. J., and Robertus, J. D. (1996) *Nat. Struct. Biol.* 3, 133-140.
11. Hollis, T., Monzingo, A. F., Bortone, K., Schelp, E., Cox, R., and Robertus, J. D. (1998) *Acta Crystallogr. D* 54, 1412-1413.
12. Koga, D., Yoshioka, T., and Arakane, Y. (1998) *Biosci., Biotechnol., Biochem.* 62, 1643-1646.
13. Fukamizo, T., Minematsu, T., Yanase, Y., Hayashi, K., and Goto, S. (1986) *Arch. Biochem. Biophys.* 250, 312-321.
14. Kuhara, S., Esaki, E., Fukamizo, T., and Hayashi, K. (1982) *J. Biochem.* 92, 121-127.
15. Davies, G. J., Wilson, K. S., and Henrissat, B. (1997) *Biochem. J.* 321, 557-559.
16. Honda, Y., and Fukamizo, T. (1998) *Biochim. Biophys. Acta* 1388, 53-65.

17. Masaki, A., Fukamizo, T., Otakara, A., Torikata, T., Hayashi, K., and Imoto, T. (1981) *J. Biochem.* **90**, 1167–1175.
18. Armand, S., Tomita, H., Heyraud, A., Gey, C., Watanabe, T., and Henrissat, B. (1994) *FEBS Lett.* **343**, 177–180.
19. Blake, C. C. F., Johnson, L. N., Mair, G. A., North, A. C. T., Phillips, D. C., and Sarma, V. R. (1967) *Proc. R. Soc. London, Ser. B* **167**, 378–388.
20. Terwisscha van Scheltinga, A. C., Armand, S., Kalk, K. H., Isogai, A., Henrissat, B., and Dijkstra, B. W. (1995) *Biochemistry* **34**, 15619–15623.
21. Brameld, K. A., Shrader, W. D., Imperiali, B., and Goddard, W. A., III (1998) *J. Mol. Biol.* **280**, 913–923.
22. Watanabe, T., Kobori, K., Miyashita, K., Fujii, T., Sakai, H., Uchida, M., and Tanaka, H. (1993) *J. Biol. Chem.* **268**, 18567–18572.
23. Usui, T., Matsui, H., and Isobe, K. (1990) *Carbohydr. Res.* **203**, 65–77.
24. Ruiz-Herrera, J., and Xoconostle-Cazares, B. (1995) *Arch. Med. Res.* **26**, 315–321.
25. Koga, D., Tsukamoto, T., Sueshige, N., Utsumi, T., and Ide, A. (1989) *Agric. Biol. Chem.* **53**, 3121–3126.
26. Hollis, T., Honda, Y., Fukamizo, T., Marcotte, E. M., and Robertus, J. D. (1997) *Arch. Biochem. Biophys.* **336**, 268–274.
27. Seigner, C., Prodanov, E., and Marchis-Mouren, G. (1985) *Eur. J. Biochem.* **148**, 161–168.
28. Malet, C., and Planas, A. (1997) *Biochemistry* **36**, 13838–13848.
29. Honda, Y., Tanimori, S., Kirihata, M., Kaneko, S., Tokuyasu, K., Hashimoto, M., Watanabe, T., and Fukamizo, T. (2000) *FEBS Lett.* **476**, 194–197.
30. Imoto, T., Johnson, L. N., North, A. C. T., Phillips, D. C., and Rupley, J. A. (1972) *Enzymes (3rd Ed.)* **7**, 665–868.
31. Brurberg, M. B., Eijsink, V. G., and Nes, I. F. (1994) *FEMS Microbiol. Lett.* **124**, 399–404.
32. Chipman, D. M. (1971) *Biochemistry* **10**, 1714–1722.

BI001537S